



Proceedings of the 3<sup>rd</sup> Conference on Nanostructures (NS2010)  
March 10-12, 2010, Kish Island, I.R. Iran

## **Proceedings**

# **The 3<sup>rd</sup> Conference on Nanostructures**

# ***NS2010***

*March 10-12, 2010*  
*Kish Island, I. R. Iran*



## Calcination Process Effect on Phase Formation in Nano-Sized Zn<sub>0.9</sub>Mn<sub>0.1</sub>O Particles

M. Ebrahimizadeh Abrishami<sup>a</sup>, S. M. Hosseini<sup>b</sup>, E. Attaran Kakhki<sup>c</sup>, A. Kompany<sup>d</sup>

<sup>a</sup>Department of Physics (Materials and Electroceramics Lab.), Ferdowsi University of Mashhad, 91775-1436, Iran, [ebrahimizadeh@ymail.com](mailto:ebrahimizadeh@ymail.com)

<sup>b</sup> Department of Physics (Materials and Electroceramics Lab.), Ferdowsi University of Mashhad, 91775-1436, Iran, [sma\\_hosseini@yahoo.com](mailto:sma_hosseini@yahoo.com)

<sup>c</sup> Department of Physics (Materials and Electroceramics Lab.), Ferdowsi University of Mashhad, 91775-1436, Iran, [Attaran\\_kak@yahoo.com](mailto:Attaran_kak@yahoo.com)

<sup>d</sup> Department of Physics (Materials and Electroceramics Lab.), Ferdowsi University of Mashhad, 91775-1436, Iran, [kompany@ferdowsi.um.ac.ir](mailto:kompany@ferdowsi.um.ac.ir)

**Abstract:** This paper reports the effects of calcination process on the structural and mid-infrared optical properties of Zn<sub>0.9</sub>Mn<sub>0.1</sub>O nanopowders synthesized by the sol gel technique. The particle size was determined about 35 nm. X-ray diffraction analysis indicated that mono-phase wurtzite structure was exhibited in samples calcinated at low temperatures. Appearance of secondary phases was well clarified that tuning the percentage of these phases can be possible by manipulating the calcination temperatures. The characterization was completed by studying the mid-infrared transmittance spectra obtained by Fourier transform infrared (FTIR) spectroscopy.

**Keywords:** Sol gel; Mn-doped ZnO; nanopowder; secondary phase

### Introduction

Zinc oxide is II-VI semiconductor stably crystallized in hexagonal (wurtzite) structure. The space group is *P63mc* and the lattice constants are about  $a=3.25\text{\AA}$  and  $c=5.21\text{\AA}$  [1]. Because of its remarkable electrical and optical properties, ZnO has attracted much more attention to use in thermoelectric [2], optoelectronic [3], electric and etc devices. Moreover, transition metal doped ZnO such as Mn, Co, Fe and Ni has been applied to fabricate Diluted Magnetic Semiconductors (DMS) as future electronics generation devices. In recent years, atom-like behaviours of nanostructures persuade researchers to synthesize nanopowders. Thus, several wet chemical methods have been suggested to prepare ZnO:Mn nanopowders such as gel combustion [4], polymerized sol gel [5], co-precipitation [6] and etc. In addition to prepare nano-scale particles, decreasing the calcination temperature, obtaining mono-phase structure, increasing Mn solubility and controlling the secondary phases are mentioned as other important aims.

In this paper, we used the sol gel method to synthesize Zn<sub>0.9</sub>Mn<sub>0.1</sub>O nanopowders. The calcination temperature effects on phase formation and lattice constants were investigated. FTIR was applied to perform a subtle analyze on secondary phase characterization and comparing the results with structural properties.

### Experimental procedures

The precursors for the synthesis of Zn<sub>0.9</sub>Mn<sub>0.1</sub>O nanoparticles were Zinc acetate dehydrate, Zn(CH<sub>3</sub>COO)<sub>2</sub>·2H<sub>2</sub>O (Merck), Manganese acetate tetrahydrate, Mn(CH<sub>3</sub>COO)<sub>2</sub>·4H<sub>2</sub>O (Merck), acetic acid (Merck) and Diethanolamine (DEA) (Merck). Zinc and

appropriate amount of manganese acetate were dissolved in a mixture of isopropanol and distilled water by magnetic stirring and heating at 40°C for 30 minutes. Then the mixture consisted of acetic acid and DEA was added to materials solution. The whole solution was constantly stirred for 10 min to become clear with no precipitate. The molar ratios of acetic acid and DEA to cations precisely kept two and unity, respectively. Then, to obtain a clear sol, the whole solution with pH=7 was refluxed for 4h at 110°C. The gel was obtained with the help of a heat bath to evaporate the solvents at temperature of 80°C and then dried at temperatures of 140-150°C directly on hot plate. The resultant black powders were calcinated at 400°C, 500°C, 600°C, 700°C and 800°C in air. The heating rate of 3°/min up to calcination temperature, keeping the temperature for 2 hour and cooling down to room temperature with the rate of 2°/min were applied to prepare nanopowders.

We have studied the structural properties and optical characterization of the samples by using X-ray diffraction (XRD; model: Siemens D500) analysis, Transmitting Electron Microscopy (TEM; LEO 912AB-Germany) and transmission spectra (in the range of 400-2000 cm<sup>-1</sup>) recorded by FTIR spectrophotometer (model: Shimadzu 4300).

### Results and Discussion

#### 1- XRD analysis

Fig. 1 shows the XRD patterns of Zn<sub>0.9</sub>Mn<sub>0.1</sub>O calcinated at 400-800°C and confirms that the samples mostly crystallized in wurtzite structure. The diffraction peaks belonging to this structure are indexed in Fig.1 (a). The characteristic peaks with high intensity confirm the well

crystallization process. These mono-phasic samples calcinated at 400°C and 500°C reveal that Mn solubility in ZnO structure increases due to decreasing particle size [7]. In addition, single phase wurtzite structure was achieved at lower calcination temperatures than other studies which reports secondary phases in samples prepared with similar calcination phases in samples prepared with similar calcination conditions [8]. However, the impurity phases were slightly appeared when the calcination temperature increased to 600°C. Fig.1(c) illustrates that two other distinguishable phases crystallized in tetragonal and cubic structure are developed. In this figure, the secondary phases' diffraction peaks are marked with "T" and "C" as meaning of tetragonal and cubic, respectively. As presented in Fig.1 (d), the tetragonal phase vigorously grows in comparison with cubic structure with increasing the calcination temperature up to 700°C. In Fig.1 (d), we have indexed the impurity peaks belonging to Zn(Mn<sub>2</sub>)O<sub>4</sub> with tetragonal symmetry and space group I4/amd. However, at calcination temperature of 800°C, we identified that the percentage of the other secondary phase with cubic symmetry and space group Fd<sub>3</sub>m clearly increased. This structure relates to Zn(Mn)O<sub>3</sub>. The percent of the secondary phase has been approximately determined from the ratio of the impurity peaks intensity to the total peaks intensity. In Fig. 2, the existence of various secondary phases for Zn<sub>0.9</sub>Mn<sub>0.1</sub>O samples calcinated at temperature range 500-800°C is summarized with the bar diagram. As calcinated temperatures starts to increase from 600°C to 700°C the portion of cubic symmetry phase reduced and the tetragonal phase increases. At calcination temperature of 800°C, this process acted vice versa.

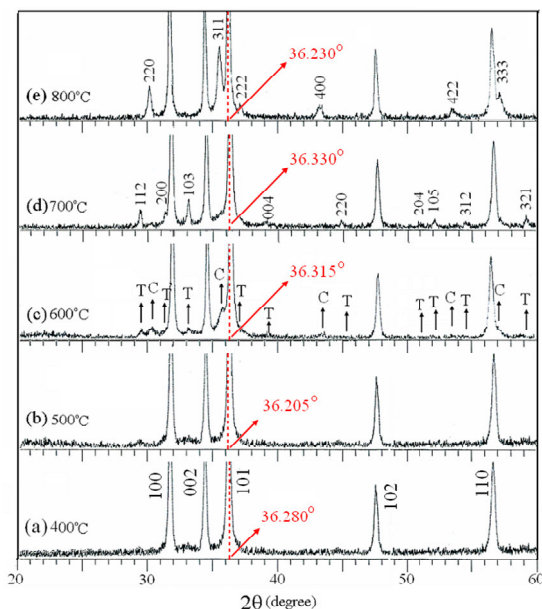


Fig. 1. XRD patterns of Zn<sub>0.9</sub>Mn<sub>0.1</sub>O calcinated at (a) 400°C, (b) 500°C, (c) 600°C, (d) 700°C, (e) 800°C. The indices in (a), (d) and (e) indicate the peak positions for the wurtzite, tetragonal and cubic structure of ZnO:Mn, respectively.

The XRD patterns presented that the wurtzite structure mostly preferred to orient in the direction of [101] peak. We have determined the intensity ratio of [101] orientation,  $i_{101}$ , to the total intensity of three other main peaks, using the formula:

$$(1) \quad i_{[101]} = \frac{I_{[101]}}{I_{[100]} + I_{[002]} + I_{[101]}} \times 100$$

The calculated values for  $i_{101}$  which are listed in table 1, clarifies that the calcination process do not effect importantly on percent of the orientations. Moreover, the guidelines in Fig. 1 illustrates the changes of [101] peak position of the nanopowders. As shown in this figure, when the calcination temperature changes from 400°C to 500°C, the peaks shift to lower angles. On the contrary, the strongest shift toward higher angles has been observed in the sample calcinated at 700°C. These shifts depend directly on the lattice constants changes as also discussed by Karamat *et al.* [9]. Provided to decreasing lattice constants, the peaks shift to higher angles. Thus, we can conclude that the decreasing lattice constants in the sample calcinated at 700°C causes the [101] peak shift toward higher angles. The measured values for lattice constants summarized in table 1, confirms this relation. This decreasing in lattice constants values in the sample calcinated at 700°C, may relates to small portion of Mn<sup>3+</sup> and Mn<sup>4+</sup> substitutions instead of Zn<sup>2+</sup>, because the ionic radius of Mn<sup>3+</sup> (0.58 Å) and Mn<sup>4+</sup> (0.53 Å) are smaller than the radius of Zn<sup>2+</sup> (0.60 Å) [10]. In proof of this conclusion, IR reflectance spectra can be applied as discussed in following results. The obtained values of structural properties are listed in table 1.

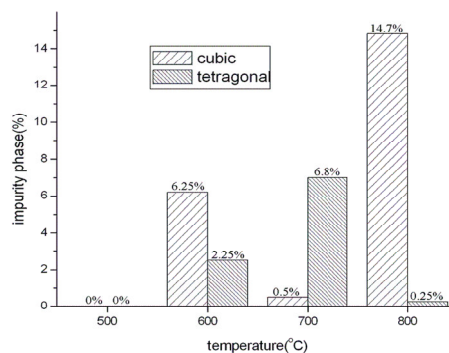


Fig. 2. Bar diagrams present an approximation on each of secondary phases' percentage in Zn<sub>0.9</sub>Mn<sub>0.1</sub>O samples calcinated at 500-800°C.

Table 1. The variations in [101] orientation percent and lattice parameters, "a" and "c" due to calcinaaion process changes.

Calcination Temperature	$i_{[101]}$	lattice const. "a" (Å)	lattice const. "c" (Å)
400°C	46.99	3.2488	5.2024
500°C	47.62	3.2534	5.2171
600°C	46.66	3.2465	5.1929
700°C	47.49	3.2491	5.1943
800°C	45.97	3.2514	5.2081

In addition, XRD spectra indicates that Full Width at Half Maximum (FWHM) of [101] peak is approximately constant in spite of the fact that calcination process were deeply changed. Thus, we deduced the average particle size constancy by using Scherrer's relation. The crystalline size calculated by this relation is 34.6 nm for the sample calcinated at 400°C which is exact in accordance with TEM result. TEM image are shown in Fig. 3 and the histogram of the particle size distribution calcinated at 400°C is presented in the inset of figure. The particles are nearly spherical shapes and the average size is estimated to be about 35 nm in diameters.

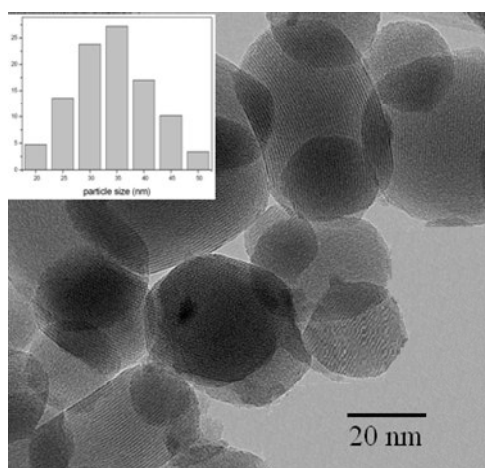


Fig.3. TEM image of  $Zn_{0.9}Mn_{0.1}O$  nanopowder calcinated at 400°C. The inset presents it's particle size distribution.

## 2- FTIR analysis

The FTIR transmission spectra of  $Zn_{0.9}Mn_{0.1}O$  with different calcination conditions are given in Fig. 4(a). The Zn-O stretching mode is clearly observed in all samples approximately centered at 480  $cm^{-1}$ . This value which shows a shift to higher wavenumbers in comparison with bulk ZnO samples [11], may depend on decreasing particle size to nano scales. However, a small deviations from 480  $cm^{-1}$  are observed in the samples contain secondary phases, due to changes in Zn-O bond length in tetragonal and cubic structure. Sometimes, the FTIR spectrum of ZnO nanopowder presents a shoulder around 510  $cm^{-1}$  as discussed by Kwon *et. al.* [12]. Hosseini *et. al.* [13] reported that this shoulder sharpened and shifted to higher wavenumbers (620-630  $cm^{-1}$ ) due to using various content of Mn as dopant. As shown in Fig.

4(a), this value for  $Zn_{0.9}Mn_{0.1}O$  calcinated at 400°C and 500°C is exactly determined at 625  $cm^{-1}$ . But, this absorption band slightly shifts to 650  $cm^{-1}$  for the sample calcinated at 700°C which has 14.7% tetragonal phase in crystallization structure. On the contrary, when the percent of cubic structure increased, the band moved from 625  $cm^{-1}$  to 615  $cm^{-1}$ . The guidelines at 480  $cm^{-1}$  and 625  $cm^{-1}$  helped us to compare between the absorption bands.

The calculated reflectance spectra of  $Zn_{0.9}Mn_{0.1}O$  calcinated at 400°C-800°C are given in Fig.4 (b). There is a strong band reflection in the range of 400-600  $cm^{-1}$  called reststrahlen band. Reststrahlen band is dominated by free carrier concentration which was not effectively changed by calcination process except in the  $Zn_{0.9}Mn_{0.1}O$  nanopowder prepared at 600°C comprising three different symmetry (wurtzite + tetragonal + cubic). Another importance in spectra is the high frequencies region dominated by valance electron concentration. Observations in Fig. 4 (b) clarifies that the reflection spectrum of  $Zn_{0.9}Mn_{0.1}O$  calcinated at 700°C shows a vigorous increase in this region which is logically concluded as adding extra electrons to the system. This result confirms the XRD analysis about small portion of  $Mn^{3+}$  and  $Mn^{4+}$  substitutions with  $Zn^{2+}$ .

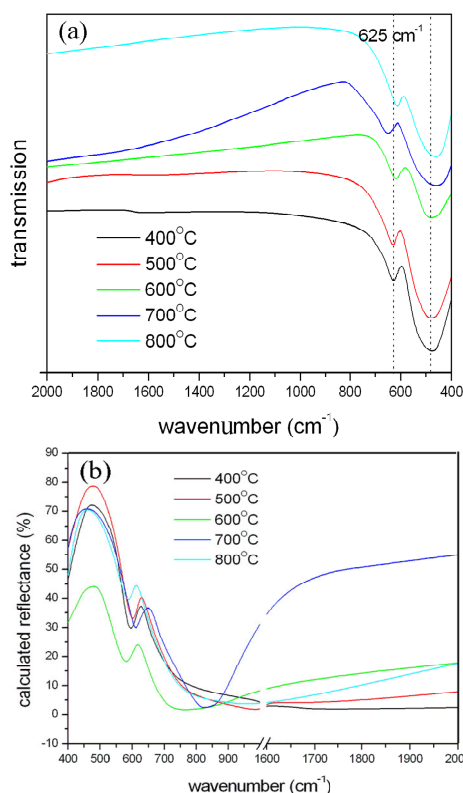


Fig. 4. (a) Transmission and (b) calculated Reflectance spectra in mid-IR region (400-2000  $cm^{-1}$ ).

## Conclusions

The  $Zn_{0.9}Mn_{0.1}O$  nanopowders were synthesized with obtaining our interesting advantages such as nano-scale



particles, mono-phasic structure at low calcination temperature, high Mn solubility and tuneable secondary phase percent. In addition, calcination process influence on mid-IR optical properties helped us to express completely a qualitative and quantitative discussion about phase investigation to confirm the structural properties extracted by XRD analysis.

effect transistors on bent flexible substrates”, *Adv. Mater.* 20 (2008) 4557-4562.

[13] M. Ebrahimzadeh Abrishami, S. M. Hosseini, E. Attaran Kakhki, A. Kompany and M. Ghasemifard “Synthesis and structure of pure and Mn-doped zinc oxide nanopowders”, *Int. J. nanosci.* (2009) Accepted.

## References

- [1] E. H. Kisi and M. M. Elcombe “Parameters for the wurtzite structure of ZnS and ZnO using powder neutron diffraction”, *Acta. Cryst.* 45 (1989) 1867-1870.
- [2] M. Ohtaki, K. Araki and K. Yamamoto “High thermoelectric performance of dually doped ZnO ceramics”, *J. Elect. Mater.* 38 (2009) 1234-1238.
- [3] V. A. Fonoberov and A. A. Balandin “ZnO quantum dots: physical properties and optoelectronic applications”, *J. Nanoelect. and Optoelect.* 1 (2006) 19-38.
- [4] N. Riahi-Noori, R. Sarraf-Mamoory, P. Alizadeh and A. Mehdikhani “Synthesis of ZnO nanopowder by a gel combustion method”, *J. Ceram. Process. Res.* 9 (2008) 246-249.
- [5] Q. Xu, S. Zhou and H. Schmidt “Magnetic properties of ZnO nanopowders”, *J. Alloys and Compounds*, (2009) DOI: 10.1016/j.jallcom.2009.08.033.
- [6] R. S. Yadav, A. C. Pandey, S. S. Sanjaya “Optical properties of Europium doped bunches of ZnO Nanowires Synthesized by co-precipitation method”, *Chalcogenide Letters*, 6 (2009) 233-239.
- [7] B. Straumal, B. Baretzky, A. Mazilkin, S. Protasova, A. Myatiev, P. Straumal “Increase of Mn solubility with decreasing grain size in ZnO”, *J. Europ. Ceram. Soc.* 29(2009)1963-1970.
- [8] O. D. Jayakumar, H. G. Salunke, R. M. Kadam, M. Mohapatra, G. Yaswant and S. K. Kulshreshta “Magnetism in Mn-doped ZnO nanoparticles prepared by a co-precipitation method”, *Nanotechnology* 17 (2006) 1278-1285.
- [9] S. Karamat, S. Mahmood, J. J. Lin, Z. Y. Pan, P. Lee, T. L. Tan, S. V. Springham, R. V. Ramanujan and R. S. Rawat “Structural and magnetic properties of  $(\text{ZnO})_{1-x}(\text{MnO}_2)_x$  thin films deposited at room temperature”, *App. Surf. Sci.* 254 (2008) 7285-7289.
- [10] K. P. Bhatti, S. Chaudhary, D. K. Pandya and S. C. Kashyap “On the room-temperature ferromagnetism in  $(\text{ZnO})_{0.98}(\text{MnO}_2)_{0.02}$ ”, *Solid State Commun.* 136 (2005) 384-388.
- [11] P. Y. Emelie, J. D. Phillips, B. Buller and U. D. Venkateswaran “Free Carrier Absorption and Lattice Vibrational Modes in Bulk ZnO”, *J. Elect. Mater.* 35 (2006) 525-529.
- [12] S. S. Kwon, W. K. Hong, G. Jo, J. Maeng, T. W. Kim, S. Song and T. Lee “Piezoelectric effect on the electronic transport characteristics of ZnO nanowire field-